JOURNAL OF AIRCRAFT
Vol. 48, No. 3, May–June 2011

Flutter of Aircraft Wings Carrying a Powered Engine Under Roll Maneuver

A. Mazidi* and S. A. Fazelzadeh†
Shiraz University, 71345 Shiraz, Iran
and
P. Marzocca‡
Clarkson University, Potsdam, New York, 13699-5725

DOI: 10.2514/1.C031080

The flutter analysis of a swept aircraft wing-store configuration subjected to follower force and undergoing a roll maneuver is presented. Concentrated mass, follower force, and roll angular velocity terms are combined in the governing equations, which are obtained using the Hamilton's variational principle. The wing is modeled from a classical beam theory and incorporates bending-torsion flexibility. Heaviside and Dirac delta functions are used to consider the location and properties of the external mass and the follower force. Also, Peters's unsteady aerodynamic pressure loadings is considered and modified to take into account the effect of the wing sweep angle. The extended Galerkin's method is applied to convert the partial differential equations into a set of ordinary differential equations. Numerical simulations are validated with available published results. Simulation results are presented to show the effects on the wing flutter of the roll angular velocity, sweep angle, follower force, and store mass and its location. Results are indicative of the significant effect of the rigid-body roll angular velocity and the follower force on the wing-store dynamic stability. Furthermore, it is shown that the distances between the wing root and the aircraft center of gravity, acting location of the roll angular velocity, considerably affects the wing-engine flutter speed and frequency.

Nomenclature

A	=	wing cross-sectional area
b	=	wing semichord
E	=	elastic modulus
G	=	shear modulus
H	=	Heaviside function
I	=	wing cross-sectional moment of inertia
J	=	wing cross-sectional polar moment of inertia
$\hat{\mathbf{I}}, \hat{\mathbf{J}}, \hat{\mathbf{K}}$	=	unit vectors of unswept coordinate system
$\hat{\mathbf{I}}_\mathbf{0}, \hat{\mathbf{J}}_\mathbf{0}, \hat{\mathbf{K}}_\mathbf{0}$	=	unit vectors of fixed coordinate system on the aircraft center of gravity
$\hat{\mathbf{i}}, \hat{\mathbf{j}}, \hat{\mathbf{k}}$	=	unit vectors of undeformed-wing coordinate system
$\hat{\mathbf{i}}', \hat{\mathbf{j}}', \hat{\mathbf{k}}'$	=	unit vectors of deformed-wing coordinate system
k_m	=	mass radius of gyration of wing cross section
L	=	wing sectional lift
l	=	wing span
M	=	aerodynamic moment
M_e	=	engine mass
m	=	mass of the wing per unit length
P	=	nondimensional follower force
$\mathbf{R_e}$	=	engine displacement vector
R_X, R_Y, R_Z	=	distances between the aircraft center of gravity and the wing root
T	=	kinetic energy
U	=	strain energy
U_∞	=	airstream velocity
v_f	=	nondimensional flutter speed
W	=	work done by nonconservative forces
w	=	displacement in z direction
X, Y, Z	=	base coordinate system
X_e, Y_e, Z_e	=	nondimensional engine location in x, y and z directions, respectively
X_0, Y_0, Z_0	=	undeformed coordinate system located at the airplane center of gravity
x, y, z	=	undeformed swept wing coordinate system
x', y', z'	=	deformed-wing coordinate system
y_φ	=	distance between center of gravity and elastic axis of the wing
δ	=	variational operator
δ_D	=	dirac delta function
η, ξ	=	wing cross-sectional local coordinates
η_e	=	nondimensional engine mass
Λ	=	wing sweep angle
λ_n	=	induced-flow states
φ	=	twist angle
ρ	=	wing material density
ρ_∞	=	air density
Ω_y	=	nondimensional roll angular velocity
ω_f	=	flutter frequency
ω_φ	=	torsional frequency

Received 26 April 2010; revision received 5 November 2010; accepted for publication 4 January 2011. Copyright © 2011 by the American Institute of Aeronautics and Astronautics, Inc. All rights reserved, Copies of this paper may be made for personal or internal use, on condition that the copier pay the $10.00 per-copy fee to the Copyright Clearance Center, Inc., 222 Rosewood Drive, Danvers, MA 01923; include the code 0021-8669/11 and $10.00 in correspondence with the CCC.

*Ph.D. Candidate, Department of Mechanical Engineering; amazidi@shirazu.ac.ir.
†Associate Professor, Department of Mechanical Engineering; fazelzad@shirazu.ac.ir.
‡Associate Professor, Department of Mechanical and Aeronautical Engineering; pmarzocc@clarkson.edu.

I. Introduction

CIVIL and military airplane wings are subjected to a variety of nonconservative forces. Aeroelastic forces, maneuver loads, and follower forces are a few examples. Since rigid-body rotations due to maneuver angular velocities, such as the one produced by a roll maneuver, can adversely affect the aircraft aeroelastic stability region, it is critical to include maneuvering angular velocities in aeroelastic analysis. Furthermore, a wide variety of external stores, heavy engine nacelles in the case of transport aircraft, or missiles and external fuel tanks for military aircraft are usually present in typical modern aircraft configuration. The geometrical and physical parameters of such external stores have a complex influence on the flutter

characteristics of aircraft wings, primarily because of the store inertial and elastic coupling effect with the wing. Modern aircraft wings are also usually subjected to several types of follower forces produced, for example, by jet propulsion, rocket thrusts, thermal loading. The interaction between the follower forces and aerodynamics, particularly for wing-store configurations, has important effects on the aeroelastic stability of the aircraft. Consequently, for a reliable aeroelastic analysis of aircraft wings it is necessary to develop refined aeroelastic models and simulation tools accounting for the effects of external stores, follower forces, and maneuver angular velocities. Furthermore, all these conditions need to be considered simultaneously.

The wing aeroelasticity is an old and practical problem and numerous papers have been published in this field, too many to list them all. Only a few relevant contributions will be discussed next. One of the first research contributions is the paper by Goland [1] on the determination of the flutter speed for a uniform cantilever wing by integration of the differential equations of the wing motion. An extension was provided for a uniform wing with tip weight [2]. Harry and Charles [3] analyzed the flutter of a uniform wing and made a comparison between the analytical and the experimental results. The aeroelastic stability of a swept wing with tip weight for an unrestrained vehicle has been considered by Lottati [4]. In this work a composite wing was studied and it was observed that flutter occurs at a lower speed, as compared with a clean-wing configuration. Gern and Librescu [5,6] contributed to show the effects of externally mounted stores on the static and dynamic aeroelasticity of advanced swept cantilevered wings. The dynamic response of adaptive cantilevered beams carrying externally mounted stores and exposed to time-dependent external excitations has been considered by Na and Librescu [7]. Librescu and Song [8] investigated the free vibration and dynamic response to external time-dependent loads of aircraft wings carrying eccentrically located heavy stores. In these contributions the authors have modeled the wing as a thin-walled anisotropic composite beam.

Follower forces are frequently encountered in structural engineering, and they can be either static or dynamic. The study of the stability of structures under follower force systems apparently started with the work by Nikolai in the late 1920s. Since then, many elastic systems loaded by follower forces have been studied and the literature associated with the study is now very extensive [9]. Much of these works focused on the stability of beams and shells subjected to tangential follower forces. The well-known Beck's beam problem, a cantilever beam excited by an axially compressive follower force, is a commonly analyzed problem in the literature [10]. However, the literature of stability of more complex structures associated with transverse follower forces is limited. Bolotin [11] provided a general understanding of the effect of nonconservative forces on elastic systems. The lateral stability of a beam under the transverse follower force was analyzed first for a pinned configuration. The correlation between stability and quasi-stability regions of elastic and viscoelastic systems subjected to nonconservative forces was investigated by Bolotin and Zhinzher [12]. The equations for a cantilevered thin beam were derived by Kalmbach et al. [13]. In this work the possibility of controlling, through feedback, a thin-cantilevered beam subjected to a nonconservative follower force was examined. The static and dynamic instabilities of a cantilevered beam and a simply supported plate under nonconservative forces have been studied by Zuo and Schreyer [14]. For the beam model, the governing partial differential equation and associated boundary conditions of the continuous model have been solved exactly. Detinko [15] used a simple slender-beam model loaded by a transverse follower force to show that the lateral stability analysis of a beam under the follower load should include realistic amount of damping to reach a correct evaluation of the critical load.

In these contributions the effects of transverse follower forces on the elastic stability of the structures have been studied. However, much of the research in this field is on the stability of the structures subjected to different types of follower forces and there is very little literature concerned with the aeroelastic stability of such structures. It seems that the stability problem of a cantilever wing containing a mass excited by a transverse follower force and subjected to aerodynamic loads has not received much attention. Como [16] analyzed the bending-torsional stability of a cantilevered beam subjected to a lateral follower force located at the beam tip. The distributed mass and inertia properties of the beam were neglected, although a concentrated mass and inertia at the tip were included. Feldt and Herrmann [17] investigated the flutter instability of a wing containing a mass subjected to the transverse follower force at the wing tip in the presence of airflow. Only one value of the bending stiffness to torsional stiffness ratio was considered in their study, a value for which thrust is destabilizing. Their results generally did not agree with previous works. Hodges et al. [18,19] have shown the effects of the lateral follower force on flutter boundary and frequency of cantilever wings; however, in this work the effect of external concentrated mass was not included. The bending-torsional flutter characteristics of an unswept wing containing a mass arbitrarily placed under a follower force have been studied by Fazelzadeh et al. [20]. The Theodorsen unsteady aerodynamic model is used for flutter analysis. The important influence of the location and magnitude of the mass and the follower force on the flutter speed and frequency of the unswept wing was highlighted. In a subsequent work Mazidi and Fazelzadeh [21] emphasized the effects of the wing sweep angle on the flutter boundaries.

Nonconservative terms in the aeroelastic governing equations can also be caused by complex maneuvering conditions. The effect of the aircraft maneuvers on the wing instability has not been thoroughly investigated. Nonlinear equations of motion for elastic panels in an aircraft, executing a pull-up maneuver of given velocity and angular velocity, were derived by Sipcic and Morino [22]. The effect of the maneuver on the flutter speed and on the limit cycle amplitude was discussed for various load conditions. Meirovitch and Tuzcu [23,24] simulated the motion of flexible aircraft and derived a unified approach to control complex airplane maneuvers. Two flight dynamics problems including the steady level cruise and a steady level turn maneuver were considered. The aeroelastic modeling and flutter characteristics of wing-stores configuration under selected maneuvers was investigated by Fazelzadeh et al. [25,26]. They have showed that the combination of flexible structural motion and maneuver parameters affects the flutter speed of the wing-stores configuration.

According to the best of the authors' knowledge the aeroelastic modeling and flutter analysis of aircraft wings containing an arbitrarily placed powered engine and subjected to roll maneuver have not yet been addressed. This study intends to fill the gap in knowledge associated with this problem. The rest of the paper is organized as follows. In Sec. II the aeroelastic governing equations are developed, and their solution and stability analysis methodology is presented in Sec. III. Numerical simulations along with validation of the proposed model are provided in Sec. IV, and conclusive remarks are provided in the last section.

II. Governing Equations

A schematic of a roll maneuvering aircraft wing engine is presented in Fig. 1. Figure 1a shows a 3-D wing and associated coordinate systems, and Fig. 1b shows the X–Z plane section. Distances between the airplane center of gravity and the wing root and location of the acting roll angular velocity are clearly indicated in this figure. The typical wing section is represented in Fig. 1c, where y_e and z_e are the distances between the center of gravity of the engine and the elastic axis of the wing. Also, points AE, AC, cg_w, and cg_e refer to the wing elastic axes, aerodynamic center of the wing, wing center of gravity, and engine center of gravity, respectively. Because of the wing's complicated dynamics, several coordinate systems are used. A fixed coordinate system, $X_0Y_0Z_0$, is located at the airplane center of gravity. The orthogonal axes X, Y, and Z are fixed on the wing root and parallel to X_0, Y_0, and Z_0 axes, respectively. This coordinate system is called the unswept wing coordinate system and rotates with respect to inertial frame at maneuver angular velocities. Another coordinate system is the swept wing coordinate system, xyz, in which the x axis lies along the length of the undeformed wing.

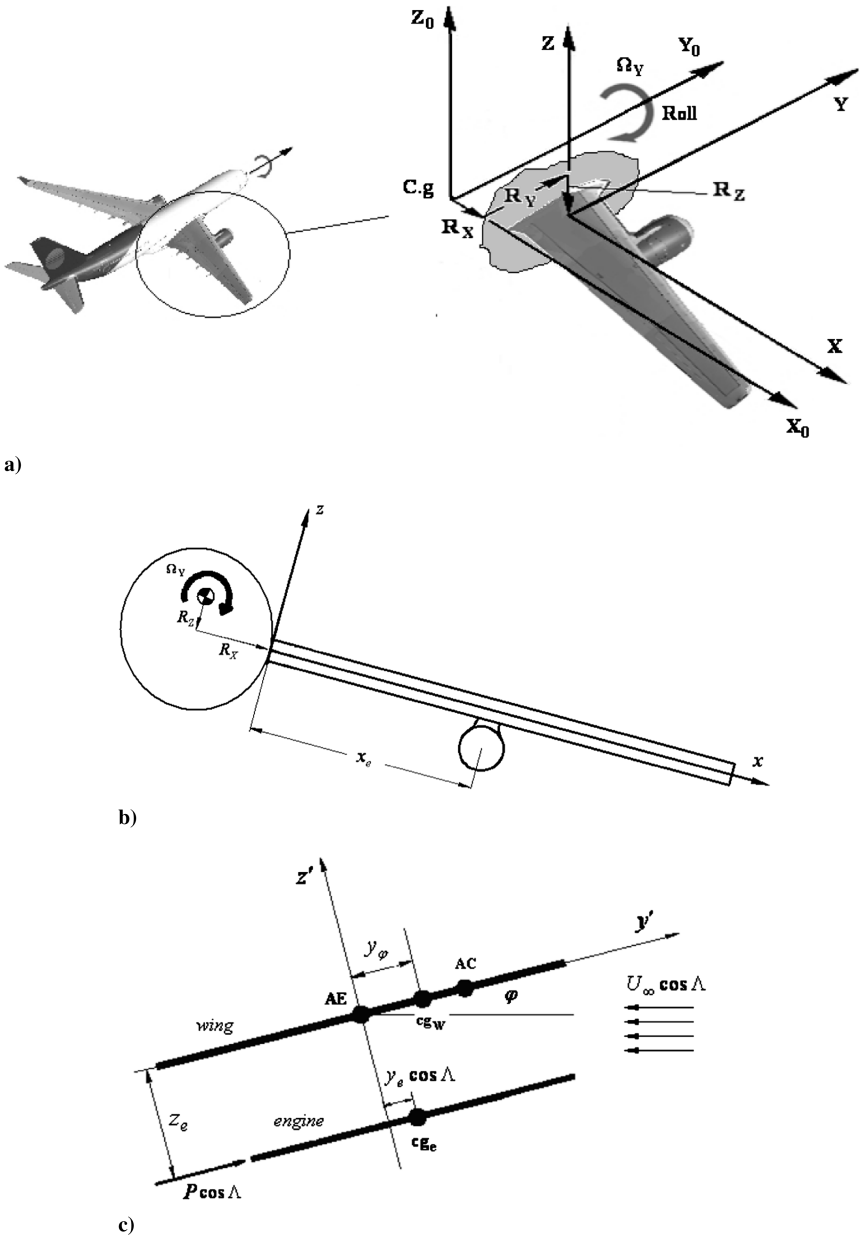

Fig. 1 Illustrations of a) coordinate systems and geometry of a swept cantilever wing engine, b) schematic of the wing in rolling maneuver, and c) wing typical section.

The last wing coordinate system is the deformed-wing coordinate system,$x'y'z'$, where x' lies along the deformed wing. After deformation, the wing shear center of the cross section located at x is displaced by an amount w in the z direction. Additionally, a cross-sectional twist angle φ about the x axis is generated. Several coordinate transformations must be used to derive the aeroelastic governing equations. Particular attention is required in the transformation from xyz to $x'y'z'$ and from XYZ to xyz. This is because all equations will be expressed in xyz coordinates, but angular velocities of maneuvering airplane are expressed in X_0, Y_0, and Z_0 coordinates. It should be noted that while deriving the kinetic energy of the wing the angular velocity vector must be first transformed into the wing coordinate system. For swept wings xyz coordinate can be achieved from X, Y, and Z by one rotation. The transformation between X, Y, and Z and x, y, and z coordinate systems is

$$\hat{i} = (\cos\Lambda)\hat{I} - (\sin\Lambda)\hat{J} \qquad \hat{j} = (\sin\Lambda)\hat{I} + (\cos\Lambda)\hat{J} \qquad \hat{k} = \hat{K} \tag{1}$$

where $\hat{i}$, $\hat{j}$, $\hat{k}$ and $\hat{I}$, $\hat{J}$, $\hat{K}$ are the unit vectors of x, y, z and X, Y, Z coordinate systems, respectively. The transformation from x, y, z to $x'y'z'$ is given by [20]

$$\hat{i}' = \hat{i} + w'\hat{k} \qquad \hat{j}' = \hat{j} + \varphi\hat{k} \qquad \hat{k}' = -w'\hat{i} - \varphi\hat{j} + \hat{k} \tag{2}$$

The equations of motion are derived using Hamilton's variational principle expressed as [27]

$$\int_{t_1}^{t_2} [\delta U - \delta T_w - \delta T_e - \delta W]\,\mathrm{d}t = 0,$$
$$\delta w = \delta\varphi = 0 \quad \text{at } t = t_1 = t_2 \tag{3}$$

where U and T are strain energy and kinetic energy, and W is the work done by the nonconservative forces. The indices w and e identify the wing and engine, respectively. The equations of motion for a wing engine under roll maneuver are obtained as [21,26]

$$m\ddot{w} + EIw'''' + my_\varphi\ddot{\varphi} + (p\sin\Lambda w' H(x_e - x) + p\cos\Lambda\varphi' H(x_e - x) - p\cos\Lambda\varphi\delta_D(x - x_e))' + (pY_e\sin\Lambda\varphi' - p\cos\Lambda\varphi + p\sin\Lambda w')\delta_D(x - x_e) + C_{ww1}\Omega_y + C_{ww2}\Omega_y^2 + (M_e\ddot{w} + M_e\ddot{\varphi}\cos\Lambda Y_e - I_{\xi_e}\ddot{w}''\sin^2\Lambda - M_e\ddot{w}'' z_e^2 - M_e Y_e^2\sin^2\Lambda\ddot{w}'' + I_{\xi_e}\ddot{\varphi}'\cos\Lambda\sin\Lambda - I_{\eta_e}\ddot{w}'' + M_e\ddot{\varphi}' Y_e^2\cos\Lambda\sin\Lambda + C_{we1}\Omega_y + C_{we2}\Omega_y^2)\delta_D(x - x_e) - L = 0 \tag{4}$$

$$I_\alpha\ddot{\varphi} + my_\varphi\ddot{w} - GJ\varphi'' + pZ_e\cos\Lambda\delta_D(x - x_e) + p\cos\Lambda(x_e - x)w''H(x_e - x) + C_{\varphi w1}\Omega_y + C_{\varphi w2}\Omega_y^2 + (I_\eta\ddot{\varphi} + I_\xi\cos^2\Lambda\ddot{\varphi} + M_e\ddot{\varphi}Z_e^2 + M_e\ddot{\varphi}\cos^2\Lambda Y_e^2 + M_e\ddot{w}Y_e\cos\Lambda - M_e\ddot{w}'\sin\Lambda Y_e^2\cos\Lambda - I_\xi\cos\Lambda\ddot{w}'\sin\Lambda C_{\varphi e1}\Omega_y + C_{\varphi e2}\Omega_y^2)\delta_D(x - x_e) - M = 0 \tag{5}$$

where C_{wwi}, C_{wei}, $C_{\phi wi}$, $C_{\phi ei}$ are roll coefficients expressed in Appendix . In Eqs. (4) and (5) the Heaviside and Dirac delta functions are used in order to accurately consider the location and properties of the thrust force and the attached mass, respectively, and the index e indicates the "engine" contributions. It should be noted here that the engine aerodynamic is not accounted for in governing equations.

The aerodynamic forces are derived from the finite-state aerodynamic model of Peters et al. [28]. Furthermore, the wing sweep angle contribution is considered by appropriate modifications in aerodynamic model, the details are reported in [21]. Therefore, the modified Peters sectional lift and aerodynamic moment modified to account for the swept angle are as follows:

$$L = \pi\rho_\infty b^2[-\ddot{w} + U_\infty\cos\Lambda\dot{\theta} - U_\infty\sin\Lambda\dot{w}' - ba(\ddot{\varphi} + U_\infty\sin\Lambda\dot{\varphi}')] + 2\pi\rho_\infty U_\infty b\cos\Lambda \times\left[-\dot{w} + U_\infty\cos\Lambda\varphi - U_\infty\sin\Lambda\dot{w}' + b\left(\frac{1}{2} - a\right)(\dot{\varphi} + U_\infty\sin\Lambda\varphi') - \lambda_0\right] \tag{6}$$

$$M = b\left(\frac{1}{2} + a\right)L - \pi\rho_\infty b^3\left[-\frac{1}{2}\ddot{w} + U_\infty\cos\Lambda\dot{\varphi} - U_\infty\sin\Lambda\dot{w}' + b\left(\frac{1}{8} - \frac{a}{2}\right)(\ddot{\varphi} + U_\infty\sin\Lambda\dot{\varphi}')\right] \tag{7}$$

where λ_0 is the induced-flow velocity. It should be noted that this model does not include drag force and it is assumed that drag effects are negligible.

III. Solution and Stability Analysis Methodology

Because of intricacy of the governing equations, it will be difficult to obtain the exact solution, therefore an approximation is obtained using the Galerkin method and procedure that lead to a residual that should be minimized in the Galerkin's sense [29]. To this end, w, φ are represented by means of series of trial functions, ψ_i that should satisfy the boundary conditions, multiplied by time-dependent generalized coordinates $\mathbf{q_i}$:

$$w = \psi_1^{\mathbf{T}}\mathbf{q_1}, \qquad \varphi = \psi_2^{\mathbf{T}}\mathbf{q_2} \tag{8}$$

The following family of functions for w and φ is used here [30]:

$$\psi_{1i} = \frac{(x/l)^{1+i}\{6 + i^2(1 - x/l)^2 + i[5 - 6x/l + (x/l)^2]\}}{i(1+i)(2+i)(3+i)}$$
$$\psi_{2i} = \mathrm{Sin}\left(\frac{i\pi x}{l}\right) \tag{9}$$

Substituting Eqs. (6–9) in Eqs. (4) and (5) and applying the Galerkin procedure on these governing equations and using the orthogonal properties in the required integrations the following set of ordinary differential equations are obtained:

$$\mathbf{M}\ddot{\mathbf{q}} + \mathbf{C}\dot{\mathbf{q}} + \mathbf{K}\mathbf{q} = 0 \tag{10}$$

Herein, $\mathbf{M}$, $\mathbf{C}$, and $\mathbf{K}$ denote the mass matrix, the damping matrix and the stiffness matrix, respectively, and $\mathbf{q}$ is the overall vector of generalized coordinates:

$$\{\mathbf{q}\} = \{\,\mathbf{q_1^T} \quad \mathbf{q_2^T}\,\}^{\mathbf{T}} \tag{11}$$

Six bending modes in the w direction, six torsion modes, and six aerodynamic states are considered in the Galerkin method to transform Eqs. (4) and (5) in a set of first-order coupled ordinary differential equations as

$$\dot{\mathbf{Z}} = [\mathbf{A}]\mathbf{Z} \tag{12}$$

The state vector $\mathbf{Z}$ is defined as

$$\mathbf{Z} = \{\,\boldsymbol{\lambda}^{\mathbf{T}} \quad \mathbf{q}^{\mathbf{T}} \quad \dot{\mathbf{q}}^{\mathbf{T}}\,\}^{\mathbf{T}} \tag{13}$$

where $\boldsymbol{\lambda}$ is the vector of induced-flow states and the system matrix $[\mathbf{A}]$ has the form

$$[\mathbf{A}] = \begin{bmatrix} [\mathbf{0}] & [\mathbf{I}] \\ -[\mathbf{M}]^{-1}[\mathbf{K}] & -[\mathbf{M}]^{-1}[\mathbf{C}] \end{bmatrix} \tag{14}$$

The problem is now reduced to the classical eigenvalue solution, to find the eigenvalues of matrix $[\mathbf{A}]$ for a given values of the air speed parameter U_∞. The eigenvalue ω is a continuous function of the air speed U_∞. For $U_\infty \neq 0$, ω is in general complex, $\omega = \mathrm{Re}(\omega) + i\mathrm{Im}(\omega)$. When $\mathrm{Re}(\omega) = 0$ and $\mathrm{Im}(\omega) \neq 0$ the wing is said to be in critical flutter condition. As U_∞ increases, $\mathrm{Re}(\omega)$ moves from negative to positive so that the motion turns from asymptotically stable to unstable.

IV. Numerical Results

The classical Goland's wing extended to variable wing sweep angles is considered. Pertinent data for this particular wing are

$m = 35.695$ kg/m, $l = 6.1$ m, $b = 0.915$ m,
$EI = 9.765 \times 10^6$ N·m^2, $GJ = 0.989 \times 10^6$ N·m^2,
$mk_m^2 = 8.694$ kg·m, $I_{M_e} = 20$ kg·m, $y_\varphi = 0.183$ m,
$a = -0.34$

Also, the following nondimensional parameters are made,

$$P = \frac{pl^2}{\sqrt{GJEI_y}}, \qquad v_f = \frac{U_f}{b\omega_\varphi}, \qquad X_e = \frac{x_e}{l}$$
$$Y_e = \frac{y_e}{b}, \qquad Z_e = \frac{z_e}{b}, \qquad \eta_e = \frac{M_e}{ml}$$
$$\Omega y = \frac{\Omega_y}{\omega_\varphi}, \qquad \bar{R}_X = \frac{R_X}{b}, \qquad \bar{R}_Z = \frac{R_Z}{b}$$

Table 1 Validation of the nondimensional flutter speed for a swept clean wing

Wing sweep angle, deg	Ref. [31]	Present	Error [a], %
−30	13.3	12.31	7.4
−20	12	11.5	4
−10	11.2	11	1.7
0	10.8	10.77	0.2
10	10.9	10.84	0.5
20	11.3	11.2	0.8
30	11.9	11.8	0.8

[a]Relative error (present results minus results of [31], divided by results of [31]).

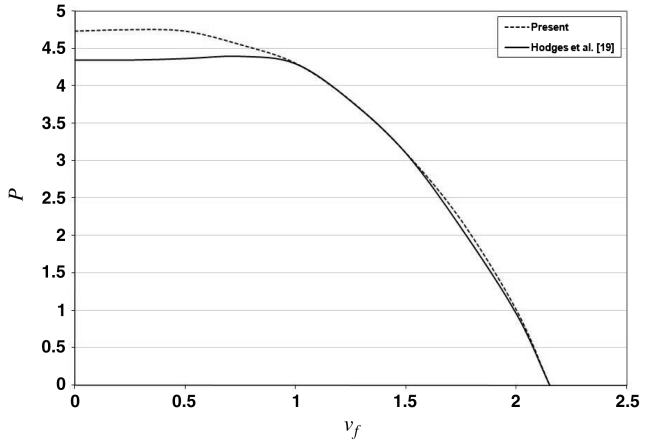

Fig. 2 Flutter boundary for an unswept clean wing subjected to thrust force.

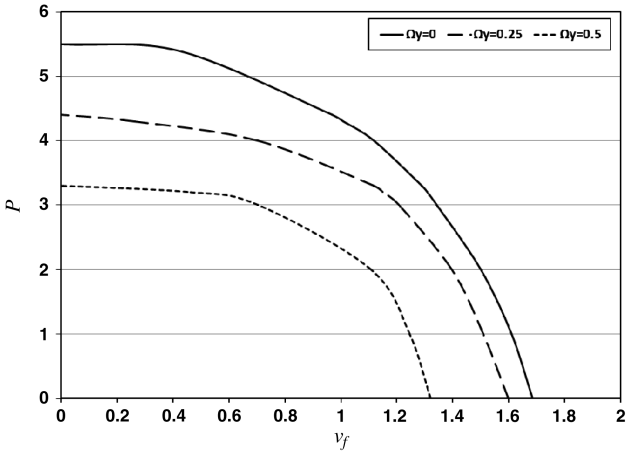

Fig. 4 Effect of the maneuver angular velocity on the wing flutter boundaries for $\eta_e = 0.5$, $X_e = 0.5$, $Y_e = -0.25$, and $\Lambda = 30$ deg.

For the purpose of model validation, the results for the swept wing without external mass are compared with Karpouzian and Librescu [31] and good agreement is reported in the range of $-10 < \Lambda < 30$ (see Table 1). Outside this range a small differences is visible and is due to the different aerodynamic model used in the two works; Peters's model is used here, and Theodorsen's model was used in [31]. It can also be seen from Table 1 that both backward and forward sweep angles significantly increase the flutter speed.

In addition, in the absence of the external mass and sweep, comparisons are also made with [19] in Fig. 2. The same wing characteristics used in this reference are selected for model validation. There are some differences between the present results and those in [19], primarily below $v_f = 1$, associated with the fact that the Galerkin method is used here, whereas the finite element method was used in the solution procedure of [19]. In the same figure the flutter boundary for a clean straight wing subjected to a lateral follower force is illustrated. A continued decrease in the flutter speed accompanying the increase in the follower force can be seen. Clearly an increase in the magnitude of the follower force is destabilizing and leads to instability at lower speeds.

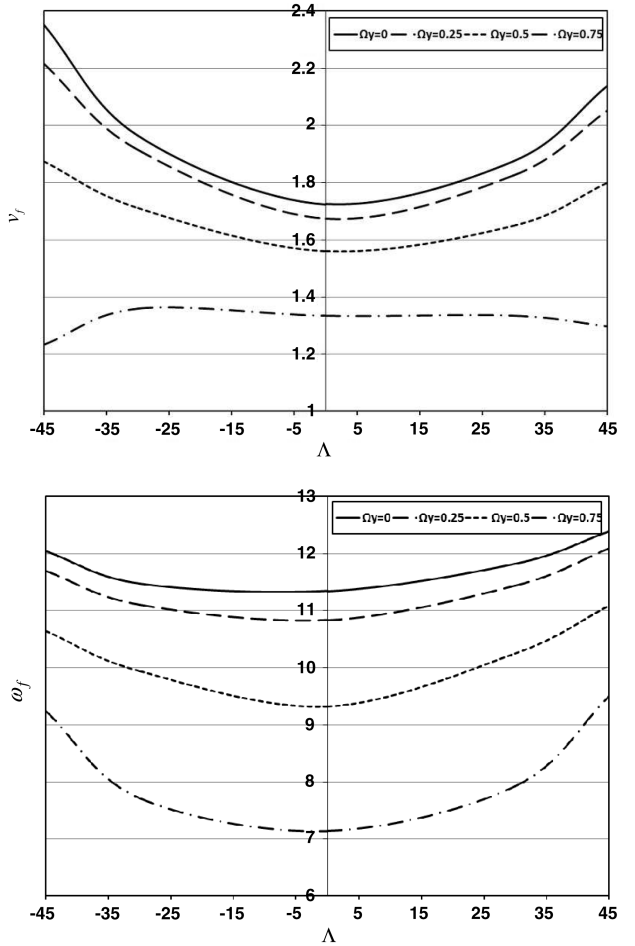

Fig. 3 Effects of the sweep angle on the clean-wing flutter boundary for selected values of roll angular velocities: a) flutter speed and b) flutter frequencies.

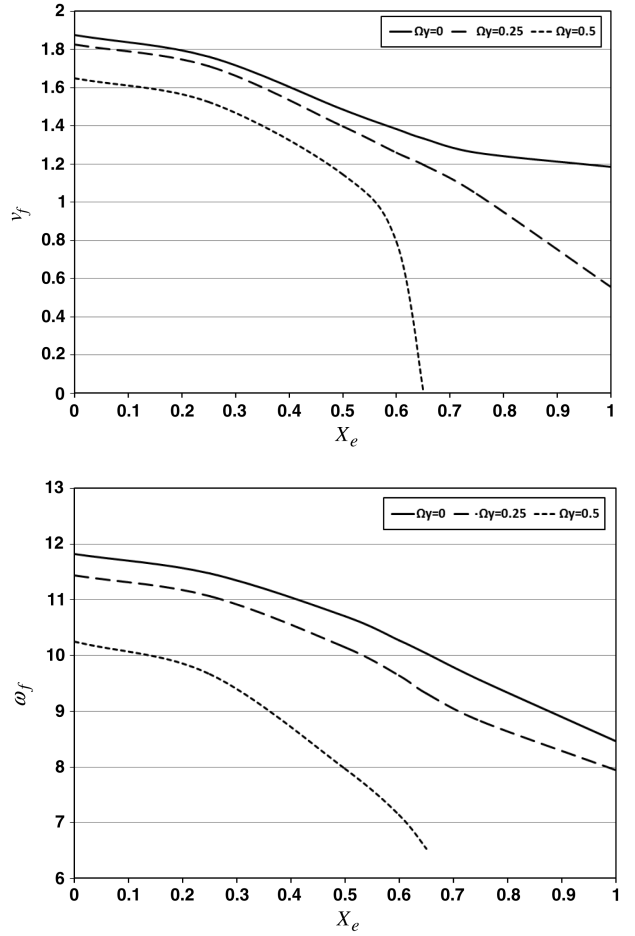

Fig. 5 Effects of the spanwise position of the engine on the wing flutter boundary for selected values of roll angular velocities and for $Y_e = -0.25$, $\eta_e = 0.5$, $\Lambda = 30$ deg, and $P = 2$: a) flutter speed and b) flutter frequencies.

Figure 3 shows the variation of the flutter speed and frequency of a clean wing for selected values of the roll angular velocity due to variations in the wing sweep angle. It can be seen from this figure that both flutter speed and frequency significantly decrease by increasing the roll angular velocity. Furthermore, both backward and forward sweep angles improve the stability domain of the wing. The trend in these figures is similar to the one reported in [5,6].

A parametric study investigating the effect of the roll angular velocity on the flutter boundary for the wing carrying a powered engine is presented in Fig. 4. The wing has a sweep angle of $\Lambda = 30$ deg. Furthermore, the engine is considered to have $\eta_e = 0.5$ and located at $X_e = 0.5$ and $Y_e = -0.25$. There is a continuous decrease in the magnitude of the thrust required for instability with an increase in airspeed. This happens because the destabilizing effect of the aerodynamic forces is added to the system, leading to instability at lower levels of the follower force. It is also clear that increasing the roll angular velocity contributes to significantly reducing the stability domain of the wing engine. This is more obvious for higher values of the roll maneuver angular velocities.

Figures 5–7 show the influence of the spanwise location of the engine on the flutter speed and frequency of the wing for different design parameters. In these figures, the engine is considered to have $\eta_e = 0.5$ and located at $Y_e = -0.25$. Figure 5 shows the variation of the flutter speed and frequency of the wing for selected values of the roll angular velocity due to variations in the spanwise location of the external mass. In this case the wing sweep angle is $\Lambda = 30$ deg and the engine thrust is $P = 2$. The effect of the roll angular velocity on the wing flutter speed is clearly highlighted. The results show that an increase of roll angular velocity can induce a lower flutter speed. This means that rolling maneuver decreases the stability domain of the airplane. For large values of the roll angular velocity the diagram coincides with zero-velocity line when the engine is located toward the wing tip. This means that rolling maneuver may lead to instability even in the absence of the air flow.

Figure 6 demonstrates the effect of the spanwise location of the powered engine on the wing flutter boundary for the selected values of the thrust force. The wing sweep angle is $\Lambda = 30$ deg and the maneuvering aircraft is considered with $\Omega_y = 0.25$. In the absence of the engine thrust, the lowest value of the flutter speed is around $X_e = 0.7$. There is a marked difference between this result and one obtained for nonmaneuvering aircraft. For the case of the wing with a mounted engine, it can be seen that increasing the distance of the engine from the wing root will decrease the flutter speed. This is more apparent for greater values of the engine thrust. The flutter speed drops to zero for large values of the engine thrust when the engine is located toward the wing tip. This can be qualitatively explained as the increase of the destabilizing effect of the engine mass and thrust leading to instability, even at zero air speed.

Effects of the spanwise location of the engine on the wing stability region for selected values of the wing sweep angle are shown in Fig. 7. The engine thrust is again $P = 2$ and the maneuvering aircraft is considered with $\Omega_y = 0.25$. Results indicate that the engine mounting location considerably affects the dynamic stability of the wing. It can be seen in Fig. 7a that increasing the distance of the engine from the wing root will decrease the flutter speed. Figure 7b also reveals that the flutter frequency drops by moving the engine towards the wing tip. In addition, effects of the wing sweep angle on the wing flutter speed and frequency is highlighted. Results show

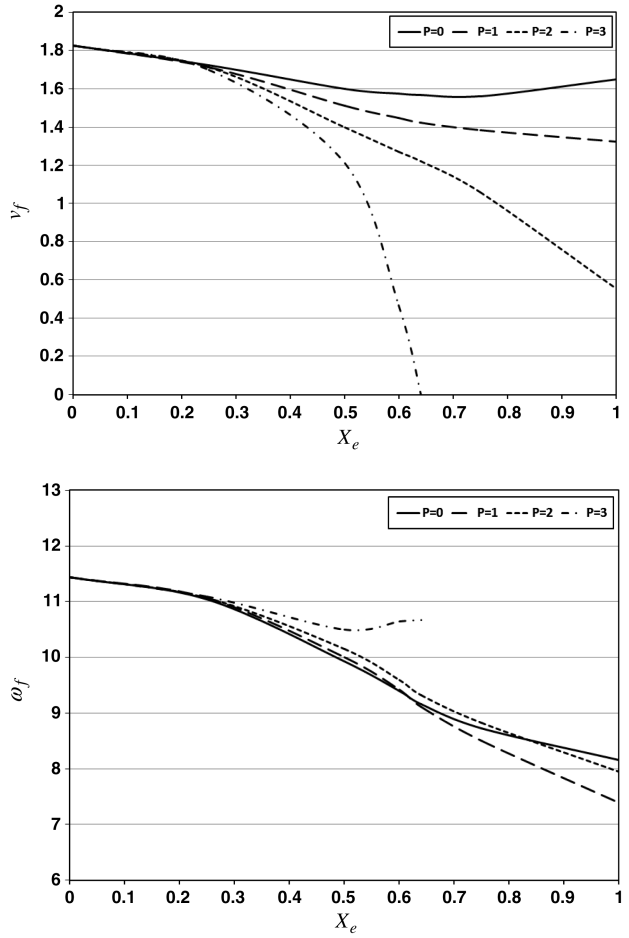

Fig. 6 Effects of the spanwise position of the engine on the wing flutter boundary for selected values of thrust forces and for $Y_e = -0.25$, $\eta_e = 0.5$, $\Lambda = 30$ deg, and $\Omega_y = 0.25$: a) flutter speed and b) flutter frequencies.

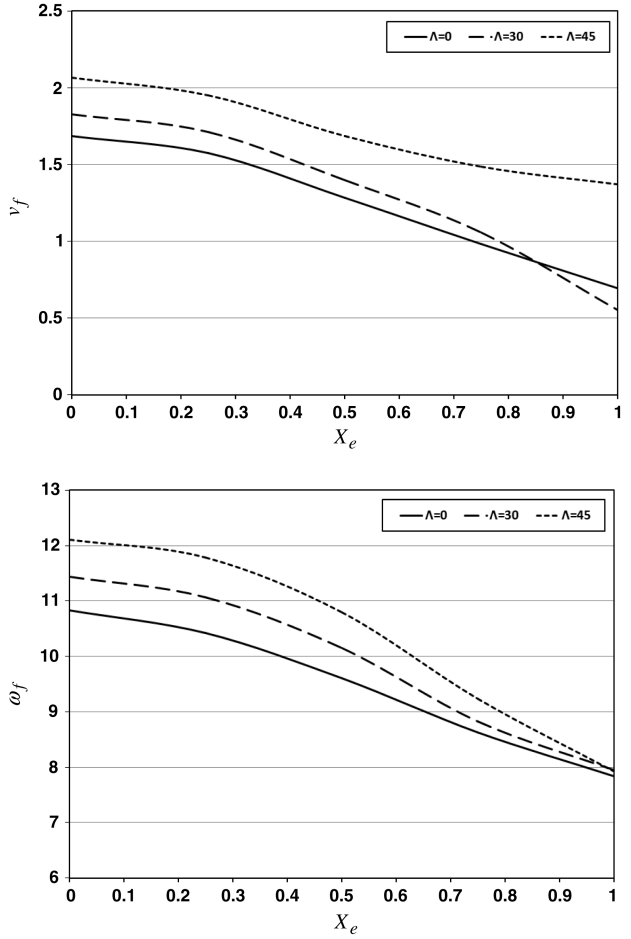

Fig. 7 Effects of the spanwise position of the engine on the wing flutter boundary for selected values of the wing sweep angle and for $Y_e = -0.25, \eta_e = 0.5, P = 2$, and $\Omega_y = 0.25$: a) flutter speed and b) flutter frequencies.

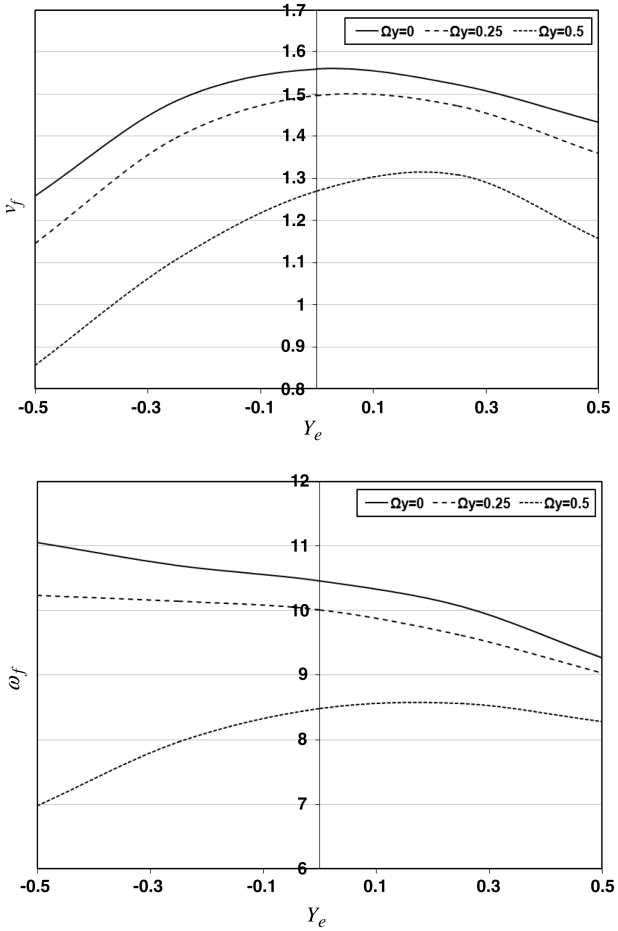

Fig. 8 Effects of the chordwise position of the engine on the wing flutter boundary for $X_e = 0.5$, $\Lambda = 30$ deg, $P = 2$, and $\eta_e = 0.5$: a) flutter speed and b) flutter frequencies.

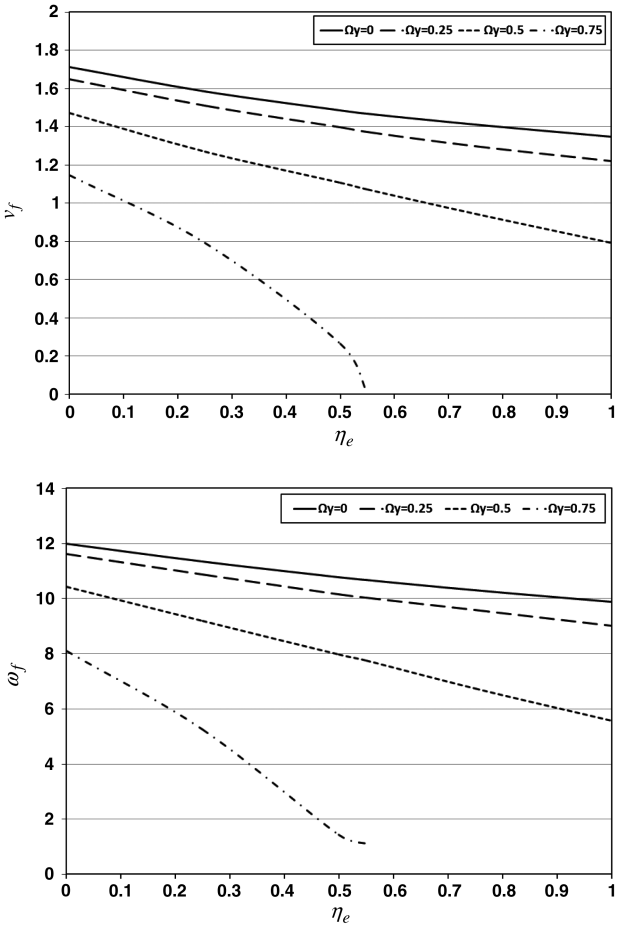

Fig. 9 Effects of the engine mass ratio on the wing flutter boundary for $X_e = 0.5$, $Y_e = -0.25$, and $P = 2$: a) flutter speed and b) flutter frequencies.

continued increase of flutter speed and frequency with increased sweep angle. This means that the wing sweep angle could positively affect the aeroelastic performance of the wing.

Figure 8 demonstrates the influence of the chordwise location of the engine on flutter speed and the frequency of the wing for different values of the roll maneuver angular velocity. The engine is located at the middle of the wing span with $\eta_e = 0.5$. Moreover, the wing sweep angle is $\Lambda = 30$ deg and the engine thrust is $P = 2$. It can be seen that the engine chordwise location contributes considerably on the wing-engine stability. When the engine is located toward the leading edge of the wing there is an increases the flutter speed, in the case of the wing carrying the engine without the follower force. However, it is evident that the flutter speed decreases in both positive and negative region of the diagram due to the presence of the follower force on the engine. Indeed, increasing the distance of the engine from the wing elastic axes in chordwise direction increases the destabilizing effects of the follower force and consequently decreases the flutter speed. Although, this is true for all values of the roll angular velocity, the stability domain is dramatically restricted by increasing the maneuver angular velocity. Furthermore, as is shown in Fig. 8b, when the engine is located toward the leading edge of the wing the flutter frequency decreases for normal maneuvering angular velocities. This behavior is dependent, obviously, on the value of the roll angular velocity. For higher values of the maneuvering angular velocities different behaviors can be seen in both flutter speed and frequency diagrams.

Figures 9 shows the effects of the engine mass on the flutter speed and frequency of the swept wing for different roll angular velocity values. The engine is located at the middle of the wing span and $Y_e = -0.25$. Also in this case, the wing sweep angle is $\Lambda = 30$ deg and the engine thrust is $P = 2$. Results show that the engine mass decreases the flutter speed and plays a destabilizing role in the dynamic stability of the wing. For high roll angular velocity values, increasing the engine mass may lead to instability at zero air speed. This means that increasing the engine mass increases the destabilizing effects of the roll maneuver. Furthermore, the effects of the roll angular velocity on the wing flutter speed and frequency can also be observed in this figure. As expected, by increasing the roll angular velocity both the flutter speed and the flutter frequency of the wing decrease.

As discussed precedently, the distance between the airplane center of gravity and the wing root is considered in the governing Eqs. (4) and (5). The wing root could have distances from the airplane center of gravity. This distance is usually neglected in the specialized literature, usually the wing is modeled as a cantilever beams with one fixed end. However, more realistically the aircraft wings supports move due to the translational and rotational motions. Because the aircraft translational and angular velocities and accelerations act on its center of gravity, distances between this point and the wing root have considerable role in finding translational and angular velocities and accelerations of the wing root. This fact implies that a reliable analysis and design of aircraft wings necessitate the development of a refined simulation model featuring the incorporation of this distance.

Influence of this contribution on the wing-engine flutter speed and frequency is studied in Figs. 10 and 11. A wing mounted engine is assumed to have $Y_e = -0.25$, $\eta_e = 0.5$, $P = 2$ and located at the middle of the wing span. Furthermore, the wing sweep angle is $\Lambda = 30$ deg. It should be noted that due to the nature of the roll maneuver, R_Y does not have any effect on the stability domain and in fact does not appear in the wing governing Eqs. (4) and (5). Also, as anticipated, the effects of R_X and R_Z on the wing-engine stability domain vanish in nonmaneuvering case. This behavior can be observed in both Fig. 10 and 11. Figure 10 shows the effect of R_X,

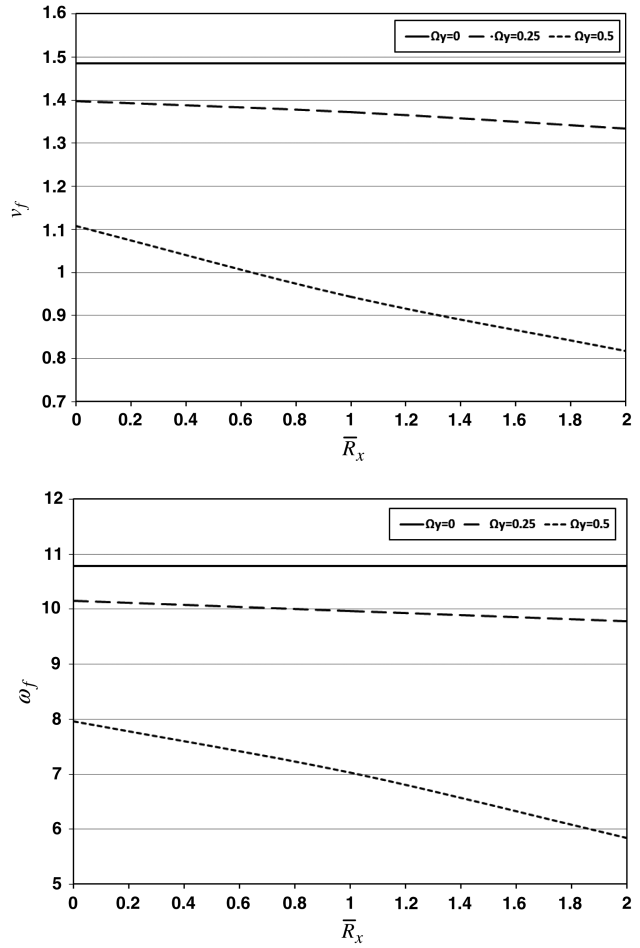

Fig. 10 Effects of the x distance between the aircraft center of gravity and the wing root on the wing flutter boundary for $X_e = 0.5, Y_e = -0.25, \eta_e = 0.5, \Lambda = 30$ deg, $P = 2$, and $\bar{R}_z = 0$: a) flutter speed and b) flutter frequencies.

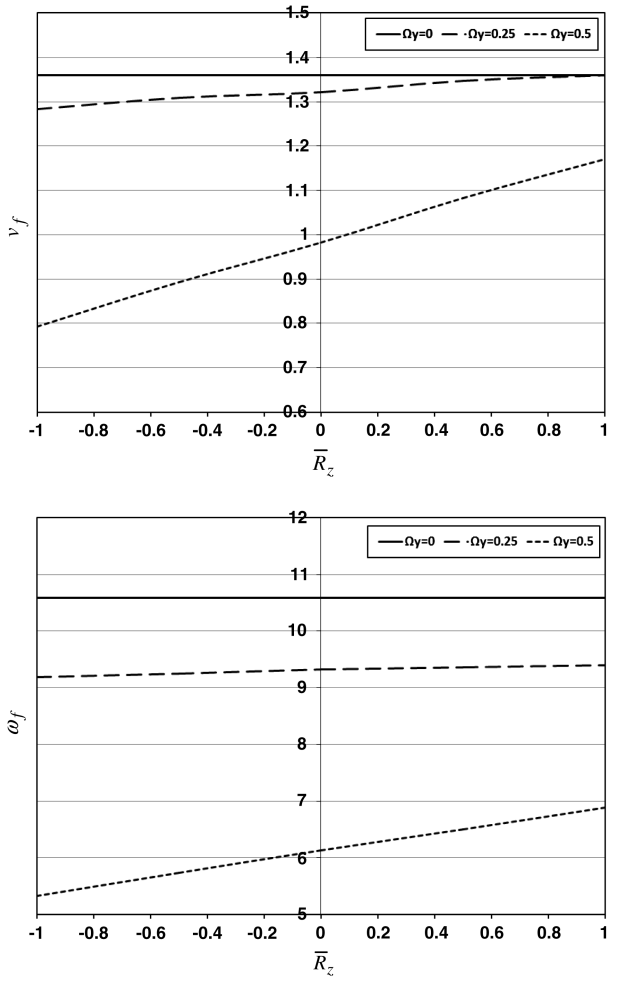

Fig. 11 Effects of the z distance between the aircraft center of gravity and the wing root on the wing flutter boundary for $X_e = 0.5, Y_e = -0.25, \eta_e = 0.5, \Lambda = 30$ deg, $P = 2$, and $\bar{R}_x = 1$: a) flutter speed and b) flutter frequencies.

distance between the aircraft center of gravity and the wing root along the X axes, on the wing-engine flutter speed and frequency for selected values of roll angular velocities. Results show that a continuous decrease in flutter speed and frequency is accompanied by the increase in R_X. This means that increasing R_X will reduce the stability domain of the system. This effect is quite small for low values of roll angular velocities and can be seen obviously for $\Omega_y = 0.5$. Because of cylindrical configuration of the airplane fuselage, upward or downward shifting the wing root related to the fuselage improves the wing-engine stability of a roll maneuvered aircraft. Figure 11 also displays the effect of R_Z, distance between the aircraft center of gravity and the wing root along the Z axes, on the wing-engine flutter speed and frequency for selected values of roll angular velocities. The wing and engine characteristics are the same as Fig. 10 and it is assumed that $\bar{R}_X = 1$. It is clear from the figure that as R_Z goes from negative to positive, an increase in the flutter speed and frequency of the wing engine is reported. This means that mounting the wing over the middle surface of the fuselage improves the stability characteristics of the wing engine. This fact is more important for higher values of the roll angular velocity, whereas for low roll angular velocities, R_Z has not a considerable effects on the flutter boundary.

V. Conclusions

The effect of one of the most popular flight maneuvers, the rolling maneuver, on flutter of an airplane wing carrying an arbitrary placed powered engine is considered. The governing equations include effects of both maneuver induced and lift and aerodynamic moment induced forces. Results are indicative of the important influence of the roll angular velocity on flutter speed and frequency of the wing engine. The results show that the rolling maneuver has a detrimental effect on the dynamic flutter and restricts the wing dynamic stability region. Because of the destabilizing effect of the maneuver induced forces, dependent to wing-engine characteristics, for large values of the roll angular velocity, the flutter may take place at zero air velocity. This is not physically achievable, since the aircraft cannot fly at speed lower than stall speed, but it shows the significant effects of the roll angular velocity on stability domain. On the other hand, increasing the rolling moment always seems to lower the flutter frequency.

Furthermore, The engine parameters, such as η_e, X_e, Y_e and the engine thrust, acts as a transverse follower force, causing remarkable changes in the wing-engine flutter speed and frequency. Clearly the effect of the roll angular velocity on the flutter speed is strongly dependent to the store mass and its location. It is found that the flutter speed and frequency in the case of a heavy store is lower than those obtained for a light one, independent of the maneuver conditions.

When distances between the airplane center of gravity and the wing root are considered in governing equations, additional insightful results are generated. R_Y does not have effect on the stability domain, however R_X and R_Z contribute considerably toward the values of the wing-engine flutter speed and frequency. For selected conditions, it is found that mounting the wing over the middle surface of the fuselage improves the wing-engine stability of a roll maneuvered aircraft.

Appendix A

$$C_{ww1} = 0$$

$$\begin{aligned}C_{ww2} &= m\sin^2\Lambda R_Z - m\cos^2\Lambda R_Z - my_\varphi \sin^2\Lambda\cos\Lambda R_X\varphi' \\ &\quad - my_\varphi\cos^3\Lambda R_X\varphi' + m\sin^2\Lambda w - m\cos^2\Lambda w \\ &\quad + m\cos^2\Lambda w'' k m_1^2 - m\cos\Lambda\sin\Lambda\varphi' k m_2^2 \\ &\quad + m\cos\Lambda\sin\Lambda\varphi' k m_1^2 + my_\varphi\sin^2\Lambda\varphi - \cos^2\Lambda my_\varphi\varphi\end{aligned}$$

$$\begin{aligned}C_{we1} &= 2M_e\sin\Lambda\dot{\varphi}Z_e + 2M_e\sin^2\Lambda\dot{\varphi}'Z_eY_e \\ &\quad + 2M_e\cos^2\Lambda\dot{\varphi}'Y_sZ_s + 4M_e\cos\Lambda\dot{w}'Z_e\end{aligned}$$

$$\begin{aligned}C_{we2} &= -M_e\sin^2\Lambda\varphi\cos\Lambda Y_e - M_e\cos^3\Lambda\varphi Y_e \\ &\quad - M_e\cos^3\Lambda\sin\Lambda Y_e^2\varphi' - M_e\cos^3\Lambda x_e\varphi' Y_s - I_{\xi_e}\cos^3\Lambda\sin\Lambda\varphi' \\ &\quad - I_{\xi_e}\sin^3\Lambda\varphi'\cos\Lambda - M_e\sin^3\Lambda\cos\Lambda Y_e^2\varphi' - I_{\eta_e}w''\sin^2\Lambda \\ &\quad + I_{\xi_e}\sin^4\Lambda w'' + M_e\cos^2\Lambda\sin^2\Lambda Y_e^2 w'' + M_e\cos\Lambda\sin\Lambda\varphi' Z_e^2 \\ &\quad + M_e\cos^2\Lambda x_e w''\sin\Lambda Y_e + M_e\sin^4\Lambda w'' Y_e^2 - M_e\sin^2\Lambda Z_e^2 w'' \\ &\quad - M_e\sin^2\Lambda Z_e - M_e\cos^2\Lambda Z_e - M_e\sin^2\Lambda w - M_e\cos^2\Lambda w \\ &\quad + I_{\eta_e}\cos\Lambda\sin\Lambda\varphi' - M_e\sin^2\Lambda R_Z - M_e\cos^2\Lambda R_Z \\ &\quad - M_e\sin^2\Lambda\cos^2\Lambda R_X Y_e\varphi' - M_e\cos^4\Lambda R_X Y_e\varphi' \\ &\quad - M_e\cos^2\Lambda R_Z Z_e w'' + M_e\sin^3\Lambda\cos\Lambda R_X Y_e w'' \\ &\quad + M_e\sin\Lambda\cos^3\Lambda R_X Z_e w'' - M_e\sin^2\Lambda R_Z Y_e\varphi'\end{aligned}$$

$$C_{\varphi w1} = 0$$

$$\begin{aligned}C_{\varphi w2} &= -I_\alpha\varphi + my_\varphi\cos\Lambda\sin^2\Lambda R_X w' + my_\varphi\cos^3\Lambda R_X w' \\ &\quad + my_\varphi\sin^3\Lambda R_X\varphi + my_\varphi\cos^2\Lambda\sin\Lambda R_X\varphi + my_\varphi\sin^2\Lambda w \\ &\quad + my_\varphi\sin^2\Lambda R_Z - my_\varphi\cos^2\Lambda R_Z + my_\varphi\cos^2\Lambda w \\ &\quad + mkm_2^2\sin\Lambda\cos\Lambda w' - mkm_1^2\sin\Lambda\cos\Lambda w' \\ &\quad + 2mkm_2^2\sin^2\Lambda\varphi - 2mkm_1^2\sin^2\Lambda\varphi - mkm_2^2\cos^2\Lambda\varphi \\ &\quad + mkm_1^2\cos^2\Lambda\varphi\end{aligned}$$

$$C_{\varphi e1} = 2M_e\cos^2\Lambda\dot{w}'Z_eY_e + 2M_e\sin^2\Lambda\dot{w}'Y_eZ_e - 2M_e\sin\Lambda\dot{w}Z_e$$

$$\begin{aligned}C_{\varphi e2} &= -M_e\sin^2\Lambda\cos^2\Lambda Y_e^2\varphi - I_\xi\varphi\cos^2\Lambda\sin^2\Lambda \\ &\quad + M_e\cos^3\Lambda x_e w' Y_e + M_e\cos^3\Lambda\sin\Lambda Y_e^2 w' \\ &\quad - I_\eta\sin\Lambda\cos\Lambda w' - M_e\sin^2\Lambda\cos\Lambda Y_e Z_e + I_\eta\varphi\cos^2\Lambda \\ &\quad - M_e\sin^2\Lambda w Y_e\cos\Lambda - M_e\cos^3\Lambda w Y_e \\ &\quad - M_e\sin\Lambda\cos\Lambda w' Z_e^2 + I_\xi\cos\Lambda\sin^3\Lambda w' \\ &\quad + I_\xi w'\cos^3\Lambda\sin\Lambda - M_e\cos^3\Lambda Z_e Y_e + M_e\sin^3\Lambda w' Y_e^2\cos\Lambda \\ &\quad - M_e\cos^4\Lambda\varphi Y_e^2 + M_e\cos^2\Lambda Z_e^2\varphi - I_\xi\cos^4\Lambda\varphi \\ &\quad + M_e\sin\Lambda\cos^2\Lambda Y_e x_e\varphi + M_e\sin\Lambda\cos\Lambda Z_e x_e \\ &\quad + M_e\sin^2\Lambda\cos^2\Lambda Y_e R_X w' - M_e\cos^3\Lambda Y_e R_Z \\ &\quad - M_e\sin^2\Lambda\cos\Lambda Y_e R_Z + M_e Z_e R_Z\varphi + M_e\sin\Lambda\cos^2\Lambda Z_e R_X \\ &\quad + M_e\sin\Lambda\cos^3\Lambda Y_e R_X\varphi + M_e\sin^3\Lambda Z_e R_X \\ &\quad + M_e\cos\Lambda\sin^3\Lambda Y_e R_X\varphi + M_e\cos^4\Lambda Y_e R_X w'\end{aligned}$$

References

[1] Goland, M., "The Flutter of a Uniform Cantilever Wing," *Journal of Applied Mechanics*, Vol. 12, 1945, pp. 197–208.

[2] Goland, M., and Luke, Y. L., "The Flutter of a Uniform Wing with Tip Weights," *Journal of Applied Mechanics*, Vol. 15, 1948, pp. 13–20.

[3] Harry, L. R., and Charles, E. W., "Flutter of a Uniform Wing with an Arbitrarily Placed Mass According to a Differential Equation Analysis and a Comparison with Experiment," NACA TN-1848, 1949.

[4] Lottati, I., "Aeroelastic Stability Characteristics of a Composite Swept Wing with Tip Weights for an Unrestrained Vehicle," *Journal of Aircraft*, Vol. 24, 1987, pp. 793–802. doi:10.2514/3.45523

[5] Gern, H., and Librescu, L., "Effect of Externally Mounted Stores on Aeroelasticity of Advanced Aircraft Wings," *Journal of Aerospace Science and Technology*, Vol. 2, 1998, pp. 321–333. doi:10.1016/S1270-9638(98)80008-4

[6] Gern, H., and Librescu, L., "Static and Dynamic Aeroelasticity of Advanced Aircraft Wings Carrying External Stores," *AIAA Journal*, Vol. 36, 1998, pp. 1121–1129. doi:10.2514/2.499

[7] Na, S., and Librescu, L., "Dynamic Response of Adaptive Cantilevers Carrying External Stores and Subjected to Blast Loading," *Journal of Sound and Vibration*, Vol. 231, 2000, pp. 1039–1055. doi:10.1006/jsvi.1999.2627

[8] Librescu, L., and Song, O., "Dynamics of Composite Aircraft Wings Carrying External Stores," *AIAA Journal*, Vol. 46, 2008, pp. 568–572. doi:10.2514/1.25541

[9] Elishakoff, I., "Controversy Associated with the So-Called 'Follower Forces': Critical Overview," *Applied Mechanics Reviews*, Vol. 58, 2005, pp. 117–142. doi:10.1115/1.1849170

[10] Beck, M., "Die Knicklast des Einseitig Eingespannten, Tangential Gedruckten Stabes," *Zeitschrift fur Angewandte Mathematik und Physik*, Vol. 3, 1952, pp. 225–288. doi:10.1007/BF02008828

[11] Bolotin, V. V., *Non-Conservative Problems of the Theory of Elastic Stability*, Pergamon, Oxford, 1963.

[12] Bolotin, V. V., and Zhinzher, N. I., "Effects of Damping on Stability of Elastic Systems Subjected to Non-Conservative Forces," *International Journal of Solids and Structures*, Vol. 5, 1969, pp. 965–989. doi:10.1016/0020-7683(69)90082-1

[13] Kalmbach, C. F., Dowell, E. H., and Moon, F. C., "The Suppression of a Dynamic Instability of an Elastic Body Using Feedback Control," *International Journal of Solids and Structures*, Vol. 15, 1974, pp. 10–36.

[14] Zuo, Q. H., and Schreyer, H. L., "Flutter and Divergence Instability of Non-Conservative Beams and Plates," *International Journal of Solids and Structures*, Vol. 33, 1996, pp. 1355–1367. doi:10.1016/0020-7683(95)00097-6

[15] Detinko, F. M., "Some Phenomena for Lateral Flutter of Beams Under Follower Load," *International Journal of Solids and Structures*, Vol. 39, 2002, pp. 341–350. doi:10.1016/S0020-7683(01)00202-5

[16] Como, M., "Lateral Buckling of a Cantilever Subjected to a Transverse Follower Force," *International Journal of Solids and Structures*, Vol. 2, 1966, pp. 515–523. doi:10.1016/0020-7683(66)90035-7

[17] Feldt, W. T., and Herrmann, G., "Bending-Torsional Flutter of a Cantilevered Wing Containing a Tip Mass and Subjected to a Transverse Follower Force," *Journal of the Franklin Institute*, Vol. 297, 1974, pp. 467–478. doi:10.1016/0016-0032(74)90123-9

[18] Hodges, D. H., "Lateral-Torsional Flutter of a Deep Cantilever Loaded by a Lateral Follower Force at the Tip," *Journal of Sound and Vibration*, Vol. 247, 2001, pp. 175–183. doi:10.1006/jsvi.2001.3624

[19] Hodges, D. H., Patil, M. J., and Chae, S., "Effect of Thrust on Bending-Torsion Flutter of Wings," *Journal of Aircraft*, Vol. 39, 2002, pp. 371–376. doi:10.2514/2.2937

[20] Fazelzadeh, S. A., Mazidi, A., and Kalantari, H., "Bending-Torsional Flutter of Wings with an Attached Mass Subjected to a Follower Force," *Journal of Sound and Vibration*, Vol. 323, 2009, pp. 148–162. doi:10.1016/j.jsv.2009.01.002

[21] Mazidi, A., and Fazelzadeh, S. A., "Flutter of a Swept Aircraft Wing with a Powered-Engine," *Journal of Aerospace Engineering*, Vol. 23, 2010, pp. 243–250. doi:10.1061/(ASCE)AS.1943-5525.0000037

[22] Sipcic, S. R., and Morino, L., "Dynamic Behavior of the Fluttering Two-Dimensional Panels on an Airplane in Pull-Up Maneuver," *AIAA Journal*, Vol. 29, 1991, pp. 1304–1312. doi:10.2514/3.10736

[23] Meirovitch, L., and Tuzcu, I., "Multidisciplinary Approach to the Modeling of Flexible Aircraft," *International Forum on Aeroelasticity and Structural Dynamics*, Madrid, 2001, pp. 435–448.

[24] Meirovitch, L., and Tuzcu, I., "Integrated Approach to the Dynamics and Control of Maneuvering Flexible Aircraft," NASA CR-2003-211748, 2003.

[25] Fazelzadeh, S. A., Mazidi, A., Rahmati, A. R., and Marzocca, P., "The Effect of Multiple Stores Arrangement on Flutter Speed of a Shear Deformable Wing Subjected to Pull-Up Angular Velocity," *The Aeronautical Journal*, Vol. 113, 2009, pp. 661–668.

[26] Fazelzadeh, S. A., Marzocca, P., Rashidi, E., and Mazidi, A., "Effects of Rolling Maneuver on Divergence and Flutter of Aircraft Wings Carrying an External Store," *Journal of Aircraft*, Vol. 47, 2010, pp. 64–70.
doi:10.2514/1.40463

[27] Baruh, H., *Analytical Dynamics*, McGraw–Hill, Boston, 1999.

[28] Peters, D. A., Karunamoorthy, S., and Cao, W. M., "Finite State Induced Flow Models; Part I: Two-Dimensional Thin Airfoil," *Journal of Aircraft*, Vol. 32, 1995, pp. 313–322.
doi:10.2514/3.46718

[29] Fletcher, C. A. J., *Computational Galerkin Methods*, Springer–Verlag, New York, 1984.

[30] Hodges, D. H., and Pierce, G. A., *Introduction to Structural Dynamics and Aeroelasticity*, Cambridge Univ. Press, Cambridge, England, U.K., 2002.

[31] Karpouzian, C., and Librescu, L., "Non-Classical Effects on Divergence and Flutter of Anisotropic Swept Aircraft Wings," *AIAA Journal*, Vol. 34, 1996, pp. 786–794.
doi:10.2514/3.13141

T. Lin
Associate Editor